ISSN 2187-0764

JAsCerS

Journal of Asian Ceramic Societies

June 2017 Vol. 5 Iss. 2

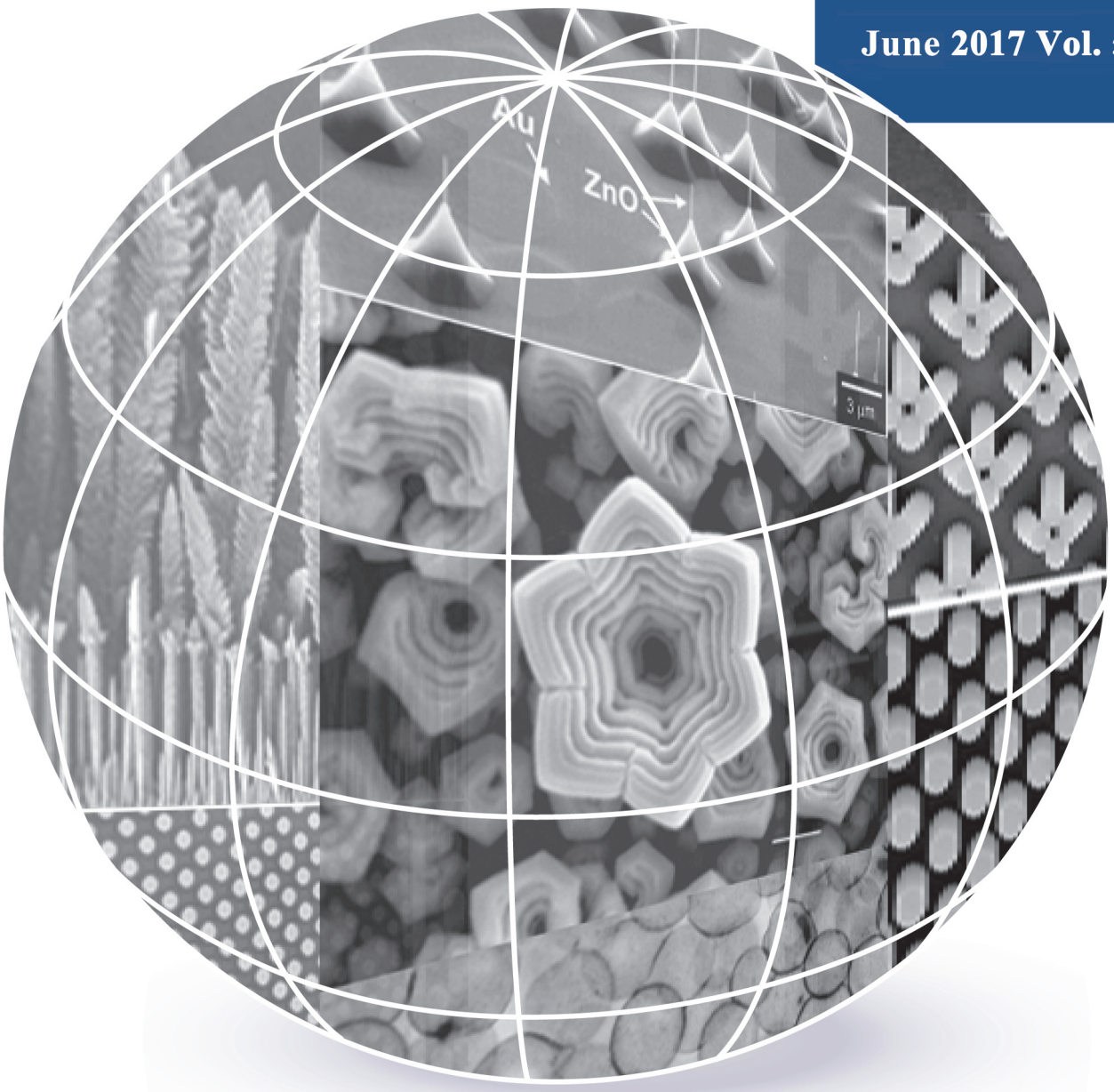

2017

Journal of Asian Ceramic Societies 5 (2017) 186–192

Contents lists available at ScienceDirect

Journal of Asian Ceramic Societies

journal homepage: www.elsevier.com/locate/jascer

Effect of alumina addition on the phase transformation and crystallisation properties of refractory cordierite prepared from amorphous rice husk silica

Simon Sembiring[a,*], Wasinton Simanjuntak[b], Rudy Situmeang[b], Agus Riyanto[a], Pulung Karo-Karo[a]

[a] Department of Physics, Faculty of Mathematics and Natural Sciences, University of Lampung, Jl. Prof. Soemantri Brojonegoro No. 1, Bandar Lampung 35145, Indonesia
[b] Department of Chemistry, Faculty of Mathematics and Natural Sciences, University of Lampung, Prof. Soemantri Brojonegoro No. 1, Bandar Lampung, 35145, Indonesia

ARTICLE INFO

Article history:
Received 18 January 2017
Received in revised form 25 April 2017
Accepted 26 April 2017
Available online 4 May 2017

Keywords:
Microstructure
Composition
Rice husk silica
Structure
Refractoriness

ABSTRACT

The effect of alumina addition of 5–30% by weight on phase transformation and crystallisation properties of refractory cordierite ceramics prepared from amorphous rice husk silica followed by sintering treatment at temperature of 1230 °C was studied. The crystallinity and microstructure of the samples were characterised using X-ray diffraction (XRD) coupled with Rietveld analysis, scanning electron microscopy (SEM), respectively. Some physical properties include density, porosity, hardness, bending strength, and thermal expansion coefficient of the samples with different alumina additions were measured. The results show that addition of alumina promoted crystallisation of cordierite into crystalline spinel, corundum, cristobalite, in which with addition of 10–30% alumina, the cordierite phase was practically undetected. Addition of alumina was also found to increase the amount of spinel, while corundum and cristobalite decreased following alumina addition of 10–30%. The presence of spinel, corundum, and cristobalite resulted in increased of density, hardness, bending strength and thermal expansion coefficient, while for porosity, the opposite was observed. Thermal expansion coefficient of the samples with alumina addition of 15–30% reach the relatively constant value of $9.5 \times 10^{-6}/^{\circ}C$, with the main crystalline phase was spinel, accompanied by corundum and cristobalite in smaller quantities.

© 2017 The Ceramic Society of Japan and the Korean Ceramic Society. Production and hosting by Elsevier B.V. This is an open access article under the CC BY-NC-ND license (http://creativecommons.org/licenses/by-nc-nd/4.0/).

1. Introduction

Rice husk has become an important and competitive source of high purity, reactive, and amorphous silica, suitable for preparation of various silica based advanced materials. In addition, this renewable agriculture residue is abundantly available in many countries around the world, ensuring its sustainability in the future. Utilisation of rice husk as a source of silica is supported by the simplicity and low cost of the extraction method of the silica. In the previous investigations, several researchers have shown that simple acid-leaching method [1–3] can be applied to obtain high purity silica, which is more advantageous compared to other conventional production techniques such as vapor phase reaction and sol–gel process applied to produce silica from other sources [4–6]. Supporting by its excellent and unique properties, such as high surface area, amorphous phase, fine particle size, and reactivity, rice husk silica has been considered as an attractive raw material for production of various advanced materials such as silicon nitride, magnesium silicide [7–9], solar grade silicon [10], silicon carbide [11], magnesium–alumina–silica [12], lithium–aluminum–silica [13], and mullite [14]. In our previous investigations, reactive silica from rice husk obtained using alkaline extraction method has been used to synthesize several ceramics materials include borosilicate [15], carbosil [16], aluminosilicate [17], mullite [18,19] and cordierite [20,21].

Of various silica based materials, cordierite ($Mg_2Al_4Si_5O_{18}$) is an important applied material in many different branches of industry due to its excellent physical properties, such as low coefficient of thermal expansion, low dielectric constant [22,23], high chemical resistance [24], excellent thermal shock resistance [25], high

* Corresponding author.
E-mail address: simon.sembiring@fmipa.unila.ac.id (S. Sembiring).

http://dx.doi.org/10.1016/j.jascer.2017.04.005
2187-0764/© 2017 The Ceramic Society of Japan and the Korean Ceramic Society. Production and hosting by Elsevier B.V. This is an open access article under the CC BY-NC-ND license (http://creativecommons.org/licenses/by-nc-nd/4.0/).

refractoriness [26], and high mechanical strength [27]. For these reasons, cordierite has been one of the most potential ceramics used in many industrial applications, such as refractory products, microelectronics, and integrated circuit board [28,29], catalyst carriers for exhaust gas purification, heat exchanger for gas turbine engines [25,30], refractory for furnaces, as well as electrical and thermal insulation [31,32]. In addition, due to its low dielectric constant and thermal expansion coefficient, cordierite is widely used as an excellent electric insulator and high-thermal resistant material. In previous studies [33,34], it was reported that thermal expansion of cordierite is $2.2 \times 10^{-6}/^{\circ}C$, while the others reported the value of around $3.3 \times 10^{-6}/^{\circ}C$ [21], $1–4 \times 10^{-6}/^{\circ}C$ [35], $0.8–2 \times 10^{-6}/^{\circ}C$ [36,37] and $2.2–4.5 \times 10^{-6}/^{\circ}C$ [38].

Refractory materials typically consist of oxides such as silicon, aluminium, magnesium, and calcium oxides. The use of these oxides is based on their high melting temperatures and the ability to form chemically bonded framework that can withstand temperatures over 1550 °C. The characteristics of refractory strongly depend on the microstructure, crystalline phase, and thermal expansion coefficient. In overall, refractory material should exhibit high thermal shock resistance, fully dense, high fracture toughness, and low thermal expansion. In our previous study [21], it was found that hardness and bending strength of refractory cordierite increased with increase in sintering temperature, while for thermal expansion coefficient, the opposite was true. Other studies [25,39] attempted to synthesize cordierite with excellent thermal shock resistance demonstrated that microstructure strongly influenced the fracture toughness and densification of cordierite.

Modifying crystal will change their physical, electrical, thermal, chemical and mechanical properties, resulting materials with superiority and unique properties. However, only limited numbers of fundamental study that have been emphasised on the cordierite crystallisation process occurring in modified composition. In previous study [40] the investigation was conducted to evaluate the synthesis of cordierite as the component of refractory material for high thermal applications by reducing the Al_2O_3 mole ratio from 2 to 1.4. They found that reduction of Al_2O_3 mole ratio to 1.4, resulted in bulk density to reach the maximum value of 2.5 kg/m^3, which is close to the value for dense cordierite ceramic. Banuraizah et al. [41] investigated the densification of cordierite and the results obtained revealed that densification process was more efficient with the presence of MgO excess up to 2.8 moles, and at the same time significantly increase the quantity of cordierite phase. Another study revealed that addition of 10% alumina resulted in increased porosity and decreased modulus of rupture, while further addition up to 30% led to decreased dielectric constant [42]. Amista et al. [43] investigated the influence of the composition on the cordierite phase and reported that stability of cordierite phase was strongly dependent on the excess of MgO and Al_2O_3. They found that the excess of MgO/Al_2O_3 led to degradation of cordierite, as suggested by the formation of forsterite and silimanite phases, and also the presence of spinel [41] and cristobalite [26]. In another study [44] it was found that increased MgO and SiO_2 contents enhanced the formation of α-cordierite, and possibly μ-cordierite, whereas increased alumina content suppressed the formation of α-cordierite and μ-cordierite.

Another scheme for composition modification of cordierite that has been attempted is addition of component other than MgO and Al_2O_3. In previous study [45] successful production of fully dense ceramic by addition of 8 wt% ZnO was reported, in which cordierite emerged as the predominant phase. Other study [46] demonstrated that crystallisation of cordierite with addition of B_2O_3, resulted in an increase in the hardness and a decrease in the thermal expansion coefficient, with the main phase of cordierite. Anwar et al. [47] reported enhanced production of dense ceramic as a result of copper addition to cordierite. Addition of copper up to 40 wt% was found to led to significant improvement of compression strength and thermal conductivity of the cordierite, while the hardness decreases. The results of several previous studies discussed above demonstrated that addition of appropriate additives can promote the formation of cordierite phase, most likely by decreasing melting point and crystallisation temperatures.

Following the successful utilisation of rice husk silica for production of refractory cordierite by thermal treatment in our previous investigation [21], this current study was aimed to expand the investigation with the emphasis on modification of composition with addition of alumina in order to explore the relationship between composition and physical characteristics of refractory cordierite. Utilisation of alumina is based on the fact that due to its excellent mechanical properties, alumina based ceramics are being increasingly used as a substitute material for several applications such as abrasive and cutting tools. The present study is concerned on the effect of Al_2O_3 (alumina) content relative to cordierite on the phase transformation, crystallisation, and physical characteristics of refractory cordierite prepared from amorphous rice husk silica. To gain insight on several basic characteristics, the crystallisation of refractory cordierite with alumina addition were studied by means of X-ray diffraction, and microstructural development of refractory cordierite by SEM studies.

2. Experimental methods

2.1. Materials

Raw husk used as a source of silica was from local rice milling industry in Bandar Lampung Province, Indonesia. Aluminum oxide (Al_2O_3) and magnesium oxide (MgO) powders with particle size 6.8–8.1 μm and purity ≥ 98.0% and absolute alcohol (C_2H_5OH) were purchased from Merck (kGaA, Damstadt, Germany). Other chemicals used were KOH 5%, HCl 5%, NaOH 5%, and distilled water.

2.2. Procedure

Synthesis of cordierite refractory using the solid-state reaction method was performed in two steps, (i) preparation of silica from rice husk, (ii) preparation of alumina-cordierite with various ratios of cordierite to alumina.

2.2.1. Preparation of silica powder from rice husk

Rice husk silica was produced using alkali extraction method following the procedure reported in previous studies [19,21]. For extraction, 50 g dried and cleaned husk was mixed with 500 ml of 5% KOH solution in a beaker glass, followed by boiling of the mixture for 30 min, and then the mixture was left overnight. The mixture was then filtered and the filtrate (silica sol) was acidified by dropwise addition of 5% HCl solution until conversion of the sol into gel was completed. The gel was oven dried at 110 °C for eight hours and then ground into powder.

2.2.2. Preparation of alumina-cordierite

Preparation of cordierite was conducted following the procedures that have previously been applied [20,21], by mixing raw materials with the composition of $MgO:Al_2O_3:SiO_2$ of 2:2:5 by mass. The solid was ground into powder by mortar and sieved to obtain the powder with the size of 200 meshes. A series of alumina-cordierite samples with mass ratios of cordierite to alumina of 100:0, 95:5, 90:10, 85:15, 80:20, 75:25 and 70:30 was prepared by mixing a specified amounts of cordierite and alumina under stirring. Each of the samples was pressed in a metal die with the pressure of 2×10^4 N/m^2 to produce cylindrical pellets and the pellets were sintered at temperature of 1230 °C according the previously known crystallisation temperature of cordierite [21], using

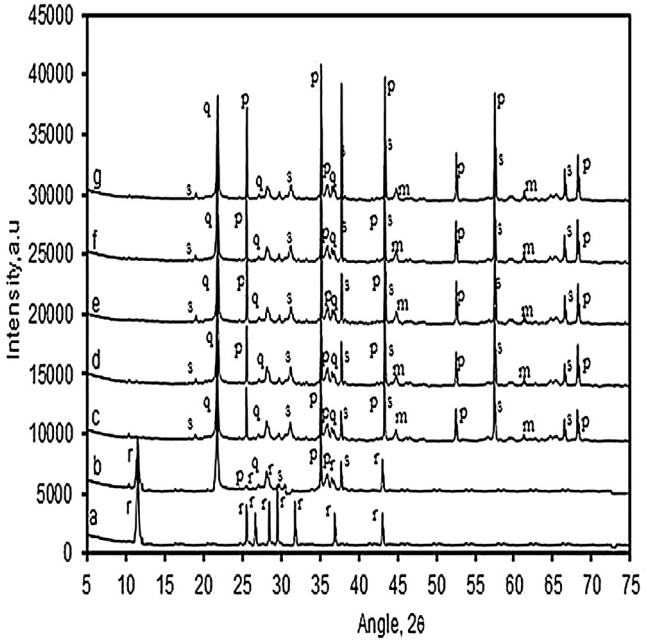

Fig. 1. The X-ray diffraction patterns of the sintered samples at temperature of 1230 °C with different alumina content (a) 0, (b) 5, (c) 10, (d) 15, (e) 20, (f) 25, and (g) 30%. p = corundum, q = cristobalite, r = α-cordierite, s = spinel, m = periclase.

temperature programmed with a heating rate of 3 °C/min and holding time of 4 h at peak temperatures.

2.2.3. Characterisation

The XRD pattens of the samples were obtained using an automated Shimadzu XD-610 X-ray diffractometer at the National Agency for Nuclear Energy (BATAN), Serpong-Indonesia operated with CuK_α radiation ($\lambda = 0.15418$) radiation in the $5^\circ \leq 2\theta \geq 80^\circ$ range, with a step size of 0.02, counting time 1s/step. The X-ray tube was operated at 40 kV and 30 mA, with a 0.15° receiving slit. The diffraction data were analysed using JADE software after subtracting the background and stripping the $CuK_{\alpha 2}$ pattern [48]. Polished and thermally etched samples were used for microstructural analysis conducted with SEM Philips-XL. Bulk density and apparent porosity were measured by Archimedes method using distilled water as liquid media [49]. Vickers hardness was measured using a Zwick tester, with three replicates measurement for each loading position. Bending strength or modulus rupture (MOR) was determined by the three-point method following the ASTM C268-70. The measuring of thermal expansion coefficient was conducted using dilatometry (Harrop Dilatometer), in the temperature range of 150–600 °C at a heating rate of 5 °C/min. The linear thermal expansion coefficient (α) was automatically calculated using the general equation: $\alpha = (\Delta L/L)(1/\Delta T)$ where: (ΔL) is the increase in length, (ΔT) is the temperature interval over which the sample is heated and (L) is the original length of the specimen.

3. Results and discussion

3.1. Effect of alumina addition on the phase transformation and crystallisation of refractory cordierite

The XRD patterns of the samples with different alumina contents after sintered at temperature of 1230 °C are presented in Fig. 1a–g. The phases identified with the PDF diffraction lines using search-match method [50], clearly show the presence of α-cordierite/$Mg_2Al_4Si_5O_{18}$ (PDF-13-0294) with the most intense peak at $2\theta = 10.50^\circ$, spinel/$MgAl_2O_4$ (PDF-21-11520), at $2\theta = 36.91^\circ$, corundum/α-Al_2O_3 (PDF-46-1212) at $2\theta = 35.12^\circ$, cristobalite/SiO_2 (PDF-39-1425), at $2\theta = 21.51^\circ$, and periclase/MgO (PDF-45-0946) at $2\theta = 42.91^\circ$.

According to Fig. 1a, the predominant crystalline phase in the sample without addition of alumina was α-cordierite and with minor crystalline phases were corundum and spinel. The profiles of crystalline phase of the samples with alumina addition are generally similar Fig. 1a–g, in term of the crystalline phases identified, except for the sample with 5% alumina addition. For this particular sample (Fig. 1b), compared to the sample without alumina addition, the intensities of peaks associated with α-cordierite and spinel decreased, whereas corundum increased, and cristobalite peaks began to appear strongly. On further increasing alumina content to 10% (Fig. 1c), α-cordierite peaks decreased significantly, but spinel, corundum, and cristobalite increased, and the new peaks of periclase was evidently exist. With increasing alumina from 15 to 30%, corundum and cristobalite peaks evidently decreased and spinel peak clearly increased. This change in phase composition suggested that increased amount of alumina led to more intensive diffusive reaction between MgO and Al_2O_3, to produce more spinel. The tendency of a this trend also indicated that binary reaction between MgO and Al_2O_3 is higher compared with binary reaction between MgO and SiO_2. This behavior was attributed to the formation of Mg–O–Al bond of spinel phase, through interaction of AlO_6 and MgO_6 octahedral [51,52,53]. These findings demonstrated that alumina tends to suppress the growth of cordierite crystals, as supported by previous study [42]. This finding is also in agreement with the result of previous study [54], in which it was suggested that the formation of spinel is most likely as a result of inter-diffusion between alumina and periclase. It was observed that the crytallisation became more intensive with increasing the alumina content. At 30% alumina addition, the sample is characterised by the presence of three distinct crystalline phases, namely spinel, corundum and cristobalite as seen in Fig. 1g. According to Rietveld analysis using the Rietica program version 1.70 [55] and Crystal Structure Database [56], the refined XRD patterns of the samples sintered at 1230 °C with the alumina content of 5 and 30% are presented in Fig. 2a and b.

The best figure of merits and weight percentage (wt%) for all samples were compiled in Table 1. The goodness of fit (GoF) values relatively low according to basic principle of GoF, in which the GoF value less than 4% and the Rwp value of less than 20% are considered acceptable [57]. As shown in Table 1, the amount of cordierite decreased as the alumina content increased from 5 to 30%, suggesting that the phase crystallisation was started by addition of 5% to produce more spinel and continued to proceed up to 30% alumina addition, which implies that more alumina reacted with a periclase to form spinel. This trend is in agreement with decreased amount of cordierite observed as the amount of alumina increased.

The surface morphologies of the samples with different alumina contents after subjected to sintering temperature of 1230 °C were analysed by SEM. The micrographs presented in Fig. 3a–g show significant effect of alumina addition on the size and distribution of the particles on the surface.

As shown in Fig. 3a–c, the surfaces morphologies of the samples are marked by the existence of particles with different grain sizes and distribution. The microstructure of the sample with 0% alumina addition (Fig. 3a) displays quite different characteristics to those of the samples with 5 and 10% alumina addition (Fig. 3b and c). The sample with 0% alumina addition (Fig. 3a) is marked by homogeneous grain size with high evident grain boundaries, and small amount of some larger grains of spinel compared to those observed for the other two samples (Fig. 3b and c). With reference to XRD results, it is obvious that the sample with 0% alumina addition is mainly composed of α-cordierite. The surfaces of the samples containing additional alumina of 5 and 10% are marked by

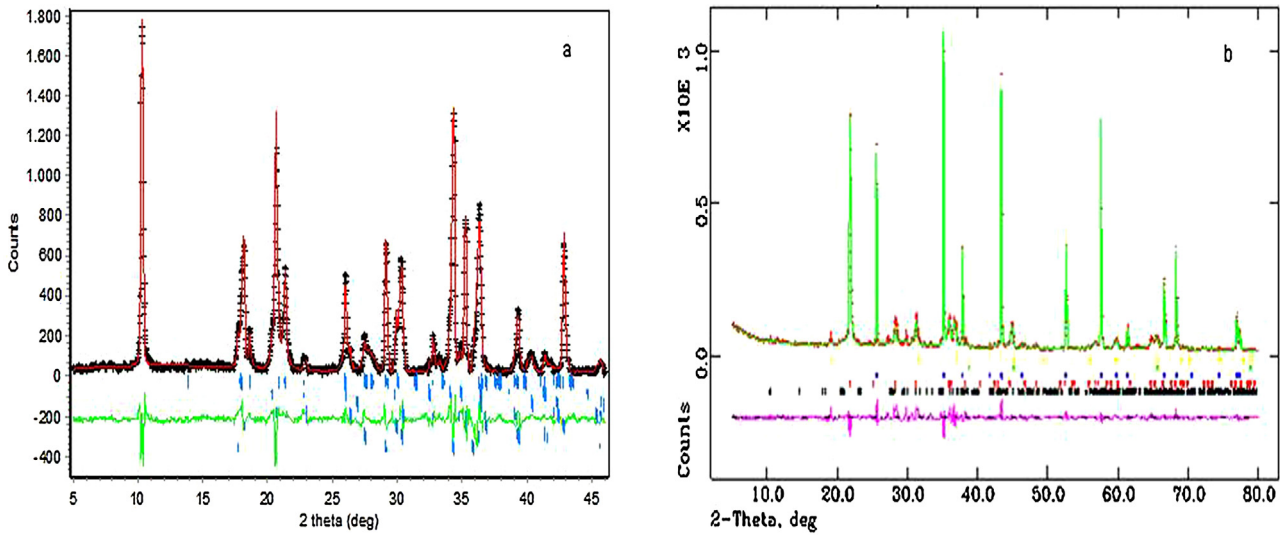

Fig. 2. XRD Rietveld of the sintered samples at temperature of 1230 °C with different alumina content (a) 5% and (b) 30%.

Table 1
Figure-of merits (FOMS) and weight percentage (wt%) from refinement of XRD data for the samples sintered at 1230 °C with different alumina addition for 6 h. Estimated errors for the least significant digits are given in parentheses. [r = α-cordierite, s = spinel, p = corundum, q = cristobalite, m = periclase].

Alumina (%)	R_{exp}	R_{wp}	R_p	GoF	r	s	p	q	m
0	9.52	10.25	11.56	1.21	90.5[3]	4.7[4]	4.8[2]	–	–
5	8.90	10.52	11.32	1.39	50.6[2]	4.1[2]	15.2[3]	30.1[4]	–
10	10.89	11.32	8.20	1.08	0.9[4]	14.5[3]	40.2[4]	42.3[2]	2.1[3]
15	11.23	11.68	8.50	1.06	0.6[2]	30.8[2]	36.9[5]	29.4[4]	2.3[2]
20	11.31	11.72	8.56	1.07	0.3[1]	36.6[2]	34.4[3]	25.3[4]	3.3[4]
25	10.61	10.92	7.92	1.06	0.4[2]	41.7[3]	31.1[5]	24.1[3]	2.7[3]
30	10.50	10.79	7.67	1.05	0.4[1]	45.4[2]	28.7[5]	22.5[4]	3.0[1]

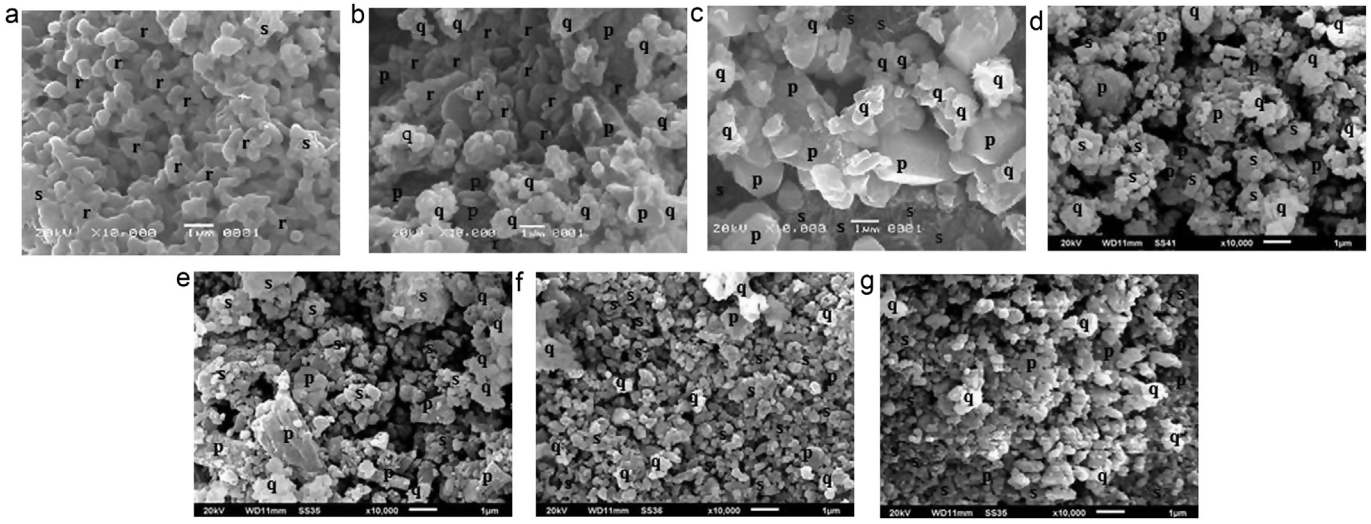

Fig. 3. The scanning electron microscopy (SEM) images of the samples sintered at 1230 °C with different alumina content (a) 0%, (b) 5%, (c) 10%, (d) 15%, (e) 20%, (f) 25%, and (g) 30%. p = corundum, q = cristobalite, r = α-cordierite, s = spinel.

fine grains of α-cordierite, covered by larger grains of spinel, corundum, and cristobalite clusters, which according to XRD results are composed of α-cordierite, spinel, corundum, and cristobalite. The presence of spinel, corundum, and cristobalite phases in the last two samples suggest that addition of alumina led to decomposition of α-cordierite, and inhibited the growth of α-cordierite phase. The above observation may be due to increased viscosity of the glassy matrix as a result of additional alumina, which suppressed the migration of atoms and inhibited the growth of cordierite. This change is supported by the results of XRD analysis presented in Fig. 1b and c.

Lower extent of α-cordierite formation was suggested by the SEM micrographs of the samples with 15–30% alumina content (Fig. 3c–g), which exhibit less agglomeration on the entire surface as the alumina content increased. This lower extent of agglomeration led to lower quantity of α-cordierite produced, as indicated by the XRD results (Table 1). This agglomeration phenomenon demonstrated that in the samples with alumina addition ranging from 15

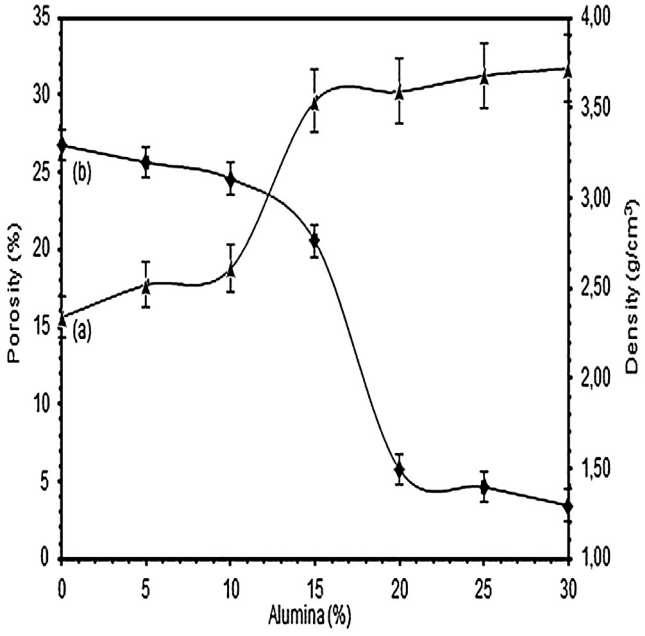

Fig. 4. Density (a) and porosity (b) of cordierite as a function of alumina addition.

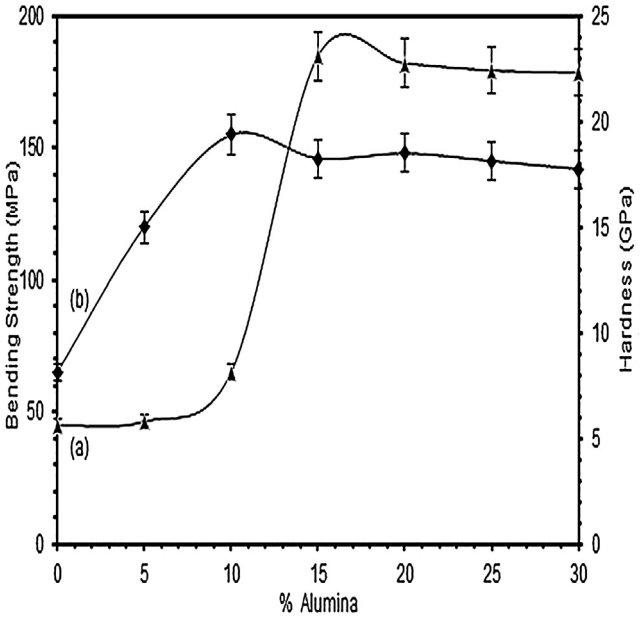

Fig. 5. Hardness (a) and bending strength (b) of cordierite as a function of alumina addition.

to 30%, the α-cordierite has decomposed completely into spinel, corundum and cristobalite. These surface characteristics suggested that at these compositions, the cordierite phase has been converted into liquefied corundum which penetrated the periclase phase, thus promoting the formation of spinel as the dominant phase, as verified By the XRD results (see Table 1). With the Rietveld calculation, it was found that the quantity of spinel increased from 30.8 to 45.4 wt% and decreased corundum and cristobalite as alumina increased from 15 to 30%.

3.2. Effect of alumina addition on the physical characteristics of refractory cordierite

The physical properties of the sintered samples at different alumina additions are shown in Figs. 4–6 .

Fig. 4 represents the variation of density and porosity with addition of alumina. It is clear that the sample without addition of alumina has the lowest density (2.34 g/cm^3) and the highest porosity (26.75%). Addition of 5% alumina causes a small increase of density to 2.52 g/cm^3, and decrease of porosity to 25.65%. Addition of 10% alumina results in a sharp increase of density (3.51 g/cm^3) but a small decrease of porosity (24.59%). This density change is most likely attributed to the increased amount of spinel and corundum phases (Table 1), while a small decrease of the porosity may be associated with relatively small difference between the densities of spinel and corundum phases.

Further addition of alumina up to 30% shows only a small increase of density but a sharp decrease of porosity (5.78%) up to 20% alumina addition and a small decrease of porosity up to 30% alumina addition. As shown in Fig. 4a, the density was slightly increased and reached the value of 3.72 g/cm^3 at alumina content of 30%. A sharp decrease of the porosity up to 20% alumina is probably due to the match between densities of spinel and corundum, whereas addition of alumina in higher quantities did not cause a remarkable decrease of porosity. Increasing the alumina content over 20% seems to suppress the pores propagation inside the matrix, causing no abrupt porosity change occurred. Although the density increased in a small extent from 15 to 30% alumina, significant change occurred in the porosity of these samples. This is due to the high density of spinel and corundum which caused density increased, and the high densities of spinel and corundum which made porosity decreased. These results are in accordance with the results of others, who reported that the density of corundum [58], spinel [59,60], and periclase [61] phases is higher than those of cordierite and cristobalite [59]. In those previous studies, the density of corundum, spinel and periclase are 3.97, 3.58 and 3.58 g/cm^3, respectively, while for cordierite and cristobalite, the reported values are 2.3 g/cm^3 and 2.6 g/cm^3 respectively. These literature data are in agreement with the findings in this present study, in which increased amount of alumina was found to enhance the formation of spinel (Table 1), as discussed above.

Fig. 5 represents the change of bending strength and hardness of the samples as a result of alumina addition.

The hardness (Fig. 5a) increased smoothly with increased alumina content from 0 to 10% and then increased sharply with alumina addition from 10 to 15%. This trend implies that the samples became highly compact and dense as a result of increased amount of alumina, increasing the ability of the sample to overcome hardness. The increase of hardness at first is referred to the large decrease of porosity. Although alumina and spinel have higher hardness than cordierite, the small porosity of sample seems to play main role in increasing its hardness. The effect alumina is obvious in cordierite with addition of alumina from 15 to 30%, in which the hardness remained constant in spite of the decrease of porosity. Practically different trend was observed for bending strength (Fig. 5b), in which sharp increase was found with alumina addition of 0–10%, followed by smooth decreased when the sample was added with 15% alumina, and relatively stable up to 30% alumina addition, as indicated by practically plat line (Fig. 5b). From practical point of view, this finding demonstrates that the hardness and bending strength of the samples are compatible with the change of density and porosity observed in this study (Fig. 4a and b). The role of density and porosity in determining hardness and bending strength is in agreement with the structure profile of the samples as revealed by the XRD results (Table 1). As previously discussed, increased amount of alumina led to formation of spinel and corundum as the prime phases. These two phases are known to have higher densities than cordierite and cristobalite, confirming the role of density in enhancing hardness of the samples, due to the change

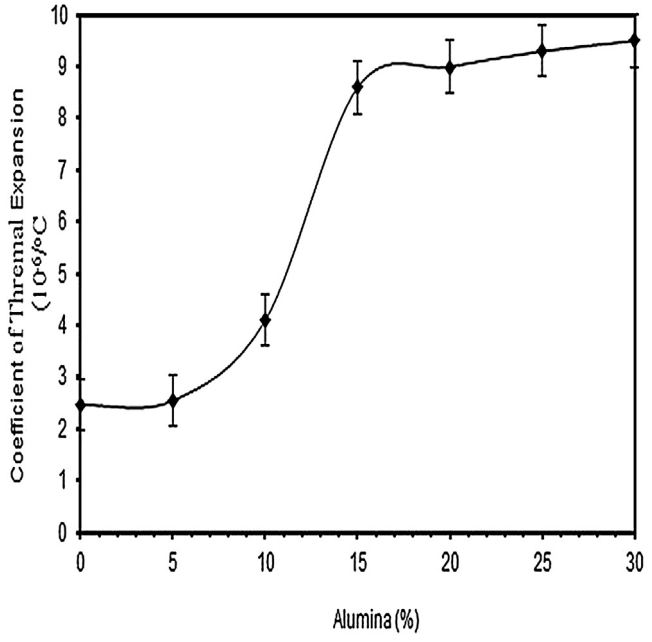

Fig. 6. Coefficient of thermal expansion of cordierite as a function of alumina addition.

in phase composition and porosity of the samples. Other factors that control the and hardness and bending strength are probably both the homogeneity and the distribution of the particles, which is in accordance with the surface morphology of the samples, as shown in Fig. 3d–g.

Fig. 6 shows the change in thermal expansion coefficient of the samples as a function of alumina addition to cordierite.

It is clearly observed that cordierite without addition of alumina has the lowest thermal expansion coefficient ($2.46 \times 10^{-6}/^{\circ}C$), and addition of 5% alumina causes a small increase of thermal expansion coefficient ($2.52 \times 10^{-6}/^{\circ}C$). The slow increase of the thermal expansion coefficient with alumina addition of 5% is attributed to the decrease of cordierite and the presence of corundum and cristobalite phases as shown in Table 1. Further addition of alumina up to 15% results in a sharp increase of the thermal expansion coefficient, and then slightly increased to the final value of $9.5 \times 10^{-6}/^{\circ}C$ at 30%. It can be deduced from the results that, as the alumina content increased, the thermal expansion coefficient increased, most probably due to the decreased amount of cordierite and increased amount of spinel (Table 1), and also decreased porosity (Fig. 4b). The trend observed in this study concerning thermal expansion coefficient is consistent with the relationship between thermal expansion coefficient with the volume fraction of the sample and porosity as described in the previous studies, in which it was explained that thermal expansion coefficient has a direct relationship with the amount of phase and an inverse relationship with the amount of the porosity [61–63], with the equation: $\alpha = (\alpha_1 v_1 + \alpha_2 v_2 + \ldots + \alpha_n v_n)(1 - P)$, where α_1, α_2 and α_n are the thermal expansion coefficients of each raw material, v_1, v_2 and v_n are the volume fractions, and P is the porosity. In this respect, for composite materials, such as ceramic, the coefficient of thermal expansion of the material is contribution of the coefficient of thermal expansion of each phase presents in the sample, depending on the value of the coefficient and volume fraction of the phase. It can be seen that coefficient of thermal expansion of spinel, corundum and periclase are higher than those of cordierite and cristobalite, which are in agreement with the results described in previous study [60]. More specifically, it was reported that the coefficient of thermal expansion of periclase [64], corundum [65], spinel [26,66] are $10.8 \times 10^{-6}/^{\circ}C$, $8.8 \times 10^{-6}/^{\circ}C$ and $9.17 \times 10^{-6}/^{\circ}C$, respectively, and cristobalite is $2.6 \times 10^{-6}/^{\circ}C$, and thermal expansion coefficient of cordierite is $2.65 \times 10^{-6}/^{\circ}C$ [26,66]. In accordance with the above values reported by others, it is clear that increased thermal expansion coefficient of the samples investigated in this study is most likely associated with increased amount of spinel and decreased amount of cordierite, as confirmed by XRD results (Table 1), also decreased porosity (Fig. 4b).

4. Conclusions

This study demonstrated that refractory cordierite was successfully produced form rice husk silica as renewable raw materials. Furthermore, the cordierite was modified by addition of varied amounts of alumina, resulting in enhanced transformation of cordierite into spinel, corundum and cristobalite. This transformation led to significant change of the characteristics of the samples, include increased density, hardness, bending strength and thermal expansion coefficient, followed by decreased porosity. Furthermore, the sample with alumina addition of 30% consists of 45.4% spinel, 28.7% corundum and 22.5% cristobalite. Thus, the samples are cordierite rich-alumina types. Based on these characteristics, it is evident that refractory cordierite of the modified samples with alumina exist as dense form with the characteristics suitable for mechanical applications, such as abrasive devices.

Acknowledgments

The authors wish to thank and appreciate the Directorate General of Higher Education (DIKTI), Ministry of Research, Technology, and Higher Education, Republic of Indonesia for research funding provided through the Competency Research Grant Program, Batch II, 2016, with contract number: 040/SP2H/LT/DRPM/II/2016 and 79/UN26/8/LPPM/2016.

References

[1] A.A.M. Daifullah, N.S. Awwad and S.A. El-Reefy, J. Chem. Eng. Process., 43, 193–201 (2004).
[2] V.P. Della, I. Kuhn and D. Hotza, Mater. Lett., 57, 818–821 (2002).
[3] K. Amutha, R. Ravibaskar and G. Sivakumar, Int. Nanotechnol. Appl., 4, 61–66 (2010).
[4] M. Tomozawa, D.L. Kim and V. Lou, J. Non-Cryst. Solids, 296, 102 (2001).
[5] P.A. Tanner, B. Yan and H. Zhang, J. Mater. Sci., 35, 4325 (2000).
[6] G. Wu, J. Wang, J. Shen, T. Yang, Q. Zhang, B. Zhou, Z. Deng, F. Bin, D. Zhou and F. Zhang, J. Non-Cryst. Solids, 275, 169 (2000).
[7] L. Sun and K. Gong, Ind. Eng. Chem. Res., 40, 5861 (2001).
[8] C. Real, M.D. Alcala and J.M. Criado, J. Am. Ceram. Soc., 79, 2012 (1996).
[9] S. Chandrasekhar, K.G. Satyanarayana, P. Pramada and T.N. Gupta, J. Mater. Sci., 38, 3159 (2003).
[10] M. Subarna, P. Banerjee, S. Purakayasha and B. Ghosh, Mater. Chem. Phys., 109, 169–173 (2008).
[11] S.K. Singh, B.C. Mohanty and S. Basu, Bull. Mater. Sci., 25, 561–563 (2002).
[12] B. Karmakar, P. Kundu, S. Jana and R.N. Dwiredi, J. Am. Ceram. Soc., 85, 2572–2574 (2002).
[13] M. Chatterjee and M.K. Naskar, Ceram. Int., 32, 623–632 (2006).
[14] M.F. Serra, M.S. Conconi, M.R. Gauna, G. Suárez, E.F. Aglietti and N.M. Rendtorff, J. Am. Ceram. Soc., 4, 61–67 (2016).
[15] S. Sembiring, Indones. J. Chem., 11, 85–89 (2011).
[16] W. Simanjuntak, S. Sembiring and K. Sebayang, J. Indones. Chem., 12, 119–125 (2012).
[17] W. Simanjuntak, S. Sembiring, P. Manurung, R. Situmeang and I.M. Low, Ceram. Int., 39, 9369–9375 (2013).
[18] S. Sembiring and W. Simanjuntak, Makara J. Sci., 16, 77–82 (2012).
[19] S. Sembiring, W. Simanjuntak, P. Manurung, D. Asmi and I.M. Low, Ceram. Int., 40, 7067–7072 (2014).
[20] W. Simanjuntak and S. Sembiring, Makara J. Sci., 15, 97–100 (2011).
[21] S. Sembiring, W. Simanjuntak, R. Situmeang, A. Riyanto and K. Sebayang, Ceram. Int., 42, 8431–8437 (2016).
[22] E. Yalamac and S. Akkurt, Ceram. Int., 32, 825–832 (2006).
[23] R. Goren, H. Gocmez and C. Ozgur, Ceram. Int., 32, 407–409 (2006).
[24] J.R. González-Velesco, R. Ferret, R. Lopez-Fonseca and M.A. Gutiérrez-Ortiz, Powder Technol., 153, 34–42 (2005).
[25] F.A.C. Oliveira and J.C. Fernandez, Ceram. Int., 28, 79–91 (2002).

[26] Z. Acimovic, L. Pavlovic, L. Trumbulovic, L. Andric and M. Stamatovic, Mater. Lett., 57, 2651–2656 (2003).
[27] A. Yamuna, S. Honda, K. Sumita, M. Yanagihara, S. Hashimoto and H. Awaji, Microporous Mesoporous Mater., 85, 169–175 (2005).
[28] A. Chowdhury, S. Mitra, S. Das, A. Sen, G.K. Samanta and P. Datta, Ceram. Int., 56, 18–22 (2007).
[29] A. Chowdhury, S. Mitra, S. Das, A. Sen, G.K. Samanta and P. Datta, Ceram. Int., 56, 98–102 (2007).
[30] P. Laokula and S. Maensirib, Adv. Sci. Technol., 45, 242–247 (2006).
[31] J.R. González-Velasco, M.A. Gutiérrez-Ortiz, R. Ferret, A. Aranzabal and J.A. Botas, Mater. Sci., 34, 1999–2002 (1999).
[32] D.L. Evans, G.R. Fischer, J.E. Geiger and F.W. Martin, J. Am. Ceram. Soc., 63, 629–634 (1980).
[33] Y. Kobayashi, K. Sumi and E. Kato, Ceram. Int., 26, 739–743 (2000).
[34] M.E. Milberg and H.D. Blair, J. Am. Ceram. Soc., 60, 372–373 (1997).
[35] A. Yamuna, R. Jhonson, Y.R. Mayajan and M. Lalithambika, J. Eur. Ceram. Soc., 24, 65–73 (2004).
[36] S. Kurama and H. Kurama, Ceram. Int., 34, 269–272 (2008).
[37] K. Zhu, Y.D. Yang, J. Wu and R. Zhang, Adv. Mater., 105–106, 802–804 (2010).
[38] E. Thomaidis and G. Kostakis, Ceram. Int., 41, 8 (2015).
[39] B.C. Lim and H.M. Jang, J. Am. Ceram. Soc., 76, 1482–1490 (1993).
[40] L. Ye, Q. Haoran, C. Xudong and Z. Ruifang, Mater. Lett., 116, 262–264 (2014).
[41] J. Banuraizah, H. Mohamad and Z.A. Ahmad, J. Am. Ceram. Soc., 94, 687–694 (2011).
[42] A.M. Salwa, A. Hameed and I.M. Bakr, J. Eur. Ceram. Soc., 27, 1893–1897 (2007).
[43] P. Amista, M. Cesari, A. Montenero, G. Gnappi and L. Lan, J. Non-Cryst. Solids, 192, 529–533 (1995).
[44] S.P. Hwang and J.M. Wu, J. Am. Ceram. Soc., 84, 1108–1112 (2011).
[45] G.H. Chen and X.Y. Liu, J. Alloys Compd., 431, 282–286 (2007).
[46] Y. Demirei and E. Gusnay, J. Ceram. Process. Res., 12, 352–356 (2011).
[47] H. Anwar, A. Al-Fouadi, R. Ola and A. Al-Rubaye, Int. J. Appl. Innov. Eng. Manage., 3, 107–112 (2014).
[48] JADE Program XRD Pattern Processing PC, Material Data Inc (MDI), Livermore, CA (1997).
[49] Australian Standard, Refractories and Refractory Material Physical Test Methods: The Determination of Density, Porosity and Water Adsorption, Australian Standard (1989), pp. 1–4, 1774.
[50] Powder Diffraction File (Type PDF-2), Diffraction Data for XRD Identification, International Centre for Diffraction Data, PA, USA (1997).
[51] R. Petrovic, D.J. Janackovič, S. Zec, S. Drmanič and L.K. Gvozdenovič, J. Sol–Gel Sci. Technol., 28, 111–118 (2003).
[52] D.J. Janackovič, V. Jokanovič, L.K. Gvozdenovic, S. Zec and D.J. Uskokovič, J. Mater. Sci., 32, 163–168 (1997).
[53] M. Okiyama, T. Fukui and C. Sakurai, J. Am. Ceram. Soc., 75, 153–160 (1992).
[54] M.K. Naskar and M. Chatterjee, J. Eur. Ceram. Soc., 24, 3499–3508 (2004).
[55] B.A. Hunter, Software Rietica for 95/98 Window NT, Version 1, 70 (1997).
[56] R.T. Downs and M. Hall-Wallase, American Mineralogist Crystal Structure Database, American Mineralogist (1997).
[57] E.H. Kisi, Mater. Forum, 18, 135–153 (1994).
[58] Aluminium Oxide (Alumina) Ceramics and Properties, Marketch International Inc (2002).
[59] I. Ganesh, Ceram. Int., 37, 2237–2245 (2011).
[60] A.H. Charles, Handbook of Ceramic Glasses and Diamonds, Mc Graw Hills, Company Inc, USA (2001).
[61] Y. Imanaka, Multilayered Low Temperature Cofired Ceramics (LTCC) Technology, Springer Science + Bussiness Media, Inc, New York, USA (2005), pp. 42–44.
[62] T. Ono, K. Matsumaru, I. Juárez-Ramírez, L.M. Torres-Martínez and K. Ishizaki, Mater. Sci. Forum, 620–622, 715–718 (2009).
[63] P. Beatrice, K. Miroslav and K. Miriam, Ceram. Silik., 46, 159–165 (2002).
[64] C.G. Kinniburgh, J. Phys. C: Solid State Phys., 9, 2692–2715 (1976).
[65] H. Schneider, K. Osaka and J.A. Pask, Mullite and Mullite Ceramics, Wiley, Chichester (1994), pp. 1–251.
[66] F. Aumento, Am. Miner., 54, 3–544 (1967).

Journal of Asian Ceramic Societies

Volume 5, Issue 2 June 2017

Available online at www.sciencedirect.com

ScienceDirect

2187-0764(201706)5:2;1-K

Journal of Asian Ceramic Societies

Volume 5, Issue 2, June 2017

The Ceramic Society of Japan and the Korean Ceramic Society.
Journal of Asian Ceramic Societies

Endorsed by the Asia-Oceania Ceramic Federation

Journal of Asian Ceramic Societies

Editorial Board

Takashi Goto
Young-Wook Kim
John Wang
Editors-in-Chief

Editorial Committee

Kunihito Koumoto
Nagoya University, Nagoya, Japan

Kazuyuki Hirao
Kyoto University, Kyoto, Japan

Takashi Goto
Tohoku University, Sendai, Japan

Suk-Joong L. Kang
KAIST, Daejeon, Korea

Hai-Doo Kim
KIMS, Changwon, Korea

Hyeong Joon Kim
Seoul National University, Seoul, Korea

Dongliang Jiang
Shanghai Institute of Ceramics, Shanghai, China

LianMeng Zhang
Wuhan University of Technology, Wuhan, China

General Editor

Takashi Goto
Tohoku University, Sendai, Japan

Editors

Yoshiyuki Sugahara
Waseda University, Tokyo, Japan

Jun-ichi Tatami
Yokohama National University, Yokohama, Japan

Takayuki Komatsu
Nagaoka University of Technology, Nagaoka, Japan

Masaru Miyayama
University of Tokyo, Tokyo, Japan

Atsunori Matsuda
Toyohashi University of Technology, Toyohashi, Japan

Shinichi Kikkawa
Hokkaido University, Sapporo, Japan

Kiyoshi Okada
Tokyo Institute of Technology, Tokyo, Japan

Katsuhisa Tanaka
Kyoto University, Kyoto, Japan

Kimihiro Yamashita
Tokyo Medical and Dental University, Tokyo, Japan

Taras Kolodiazhnyi
National Institute for Materials Science, Tsukuba, Japan

Deug Joong Kim
Sungkyunkwan University, Seoul, Korea

Jong Heo
POSTECH, Pohang, Korea

Suk-Joong L. Kang
KAIST, Daejeon, Korea

Do Kyung Kim
KAIST, Daejeon, Korea

Seong-Hyeon Hong
Seoul National University, Seoul, Korea

Yong-Ho Choa
Hanyang University, Seoul, Korea

Sahn Nahm
Korea University, Seoul, Korea

Lidong Chen
Shanghai Institute of Ceramics, Shanghai, China

Jing-Feng Li
Tsinghua University, Beijing, China

Zhengyi Fu
Wuhan University of Technology, Wuhan, China

Cewen Nan
Tsinghua University, Beijing, China

Jianrong Qiu
South China University of Technology, Guangzhou, China

Yanchun Zhou
Aerospace Research Institute of Materials and Processing, Beijing, China

Shaoming Dong
Shanghai Institute of Ceramics, Shanghai, China

Guo-Jun Zhang
Shanghai Institute of Ceramics, Shanghai, China

Shu-Hong Yu
University of Science and Technology of China, Hefei, China

Wei-Hsing Tuan
National Taiwan University, Taipei, Taiwan

Chun-Hway Hsueh
National Taiwan University, Taipei, Taiwan

Gordon Thorogood
Australian Nuclear Science and Technology Organisation
Lucas Heights, Australia

Wei Gao
University of Auckland, Auckland, New Zealand

Sam Zhang Shanyong
Nanyang Technological University, Singapore

Yi-Bing Cheng
Monash University, Australia

Lalit Mohan Manocha
Sardar Patel University, V.V. Nagar, India

Bikramjit Basu
Indian Institute of Science, Bangalore, India

Ibrahim Henk Metselaar
University of Malaysia, Kuala Lumpur, Malaysia

Roger J. Narayan
UNC/NUSU BME, Chapel Hill, USA

Walter Krenkel
University of Bayreuth, Bayreuth, Germany

Derek C. Sinclair
University of Sheffield, Sheffield, UK

Lennart Bergström
Stockholm University, Stockholm, Sweden

James Shen
Stockholm University, Stockholm, Sweden

Stuart Hampshire
University of Limerick, Limerick, Ireland

Pavol Sajgalik
Institute of Inorganic Chemistry, Bratislava, Slovakia

Paolo Colombo
University of Padova, Padova, Italy

Hasan Mandal
Sabanci University, Istanbul, Turkey